

Effect on and Correlation between Particle Size, X-ray density and Dielectric Constant, of Nanocrystalline spinel Ferrite Material due to Doping of Ni²⁺, Co²⁺ and Cu²⁺ in CuCo, NiCu and CoNi respectively prepared by Sol Gel Auto Combustion Method.

A.M. Tamboli^{1*}

Associate Professor, Department of
Electronic Science, Poona College,
Camp, PUNE-411001,
Maharashtra, INDIA¹.

Dr. S.M.Rathod³

Associate Professor, Department of
Physics, Abasaheb Garware College,
PUNE- 411 004, Maharashtra, INDIA³.

Dr. Gulam Rabbani²

Associate Professor, Department of
Physics and Electronics, Maulana Azad
College, Aurangabad,
Maharashtra, INDIA².

V.D.Kulkarni⁴

Associate Professor, Department of
Physics, Hutatma Rajguru Mahavidya,
Rajguru Nager, Dist.-PUNE,
Maharashtra, INDIA³.

Dr. Shaikh.M.Azhar⁵

Associate Professor, Department of
Physics, Sir Sayyed College of Arts,
Commerce and Science, Roshan Gate
Aurangabad, Maharashtra, INDIA³.

*Communicating Author
tambolipoona@gmail.com

Abstract—Herein the preparation of ferrite materials by using chemical reactions such as SOL-GEL Auto Combustion Technique is explained and important physical and Dielectric properties of Nanocrystalline spinel ferrite material. Structural characterization of the annealed samples at 400°C for 4 hours was done by using X-ray diffraction method (XRD). The single phase formation of NiCuCoFe₂O₄ was confirmed by X-ray diffraction analysis. The Fourier transform Infrared Spectra (FT-IR) confirmed that the synthesized material is crystalline spinel ferrite. XRD revealed that the average crystalline particle size which was calculated by using Bragg's law and Scherrer method is around 29 nm. The X-ray density is also calculated. The pellets are made from ferrite powder by using polyvinyl alcohol (PVA) as binder and by using LCR-Q meter, the Dielectric constant is calculated in the frequency range of 100Hz to 5MHz at room temperature. The effect on Particle size, X-Ray Density and Dielectric Constant is observed due to doping of Ni²⁺, Co²⁺ and Cu²⁺ in CuCo, NiCu and CoNi respectively. The correlation ship between the Particle size, X-ray density and Dielectric Constant is discussed.

Keywords- Sol-gel auto-combustion, X-ray diffraction (XRD), FT-IR, LCR-Q meter.

I. INTRODUCTION

Nanocrystalline Materials have become a subject of considerable interest in last few decades and many physical studies have been devoted to them. The ability to produce nanosized due to small grain size which changes the magnetic, dielectric and resistivity properties and opened new application for materials such as magnetic data storage, strong magnetron in electronics, Ferro fluid technology, magnetically targeted drug carriers, filters in electronic communication and agents in magnetic resonance imaging.

Nano-ferrites form an important class of Nanocrystalline materials because of their low weight, high resistivity and low energy losses (eddy current) and hence have vast technological application over wide range of frequencies [1-2]. Recent studies have shown that the physical properties of nanoparticles are influenced significantly by the processing technique [3-4]. Since crystallite size, distribution of particle sizes and inter particle spacing have the greatest impact on AC conductivity and Dielectric properties. Many wet-chemical methods are employed for the preparation of the nano-sized spinel ferrite. One of them is sol-gel auto combustion which has recently become very popular technique. It is a simple process, which offers significant saving in time and energy consumption over

the traditional methods and requires a low sintering temperature. This method is used to obtain improved properties, more homogeneity and narrow particle distribution thereby influencing structural, electrical and Dielectric properties of spinel ferrite [5-7]. It is well known that, some magnetic properties such as saturation magnetization and Coercivity and some Dielectric properties such as Dielectric loss tangent ($\tan \delta$), AC electrical conductivity (σ_{ac}) and Dielectric constant (Real Part = ϵ') depend strongly on the particle size and microstructure of the materials. Therefore, it is interesting and important to develop techniques by which the size and shape of the particles can be well controlled. One of the ways to prepare the nanocrystalline spinel ferrite material with required properties is Sol-gel auto combustion technique. In the present work we have systematically studied the effect of doping of Ni²⁺, Co²⁺ and Cu²⁺ in CuCo, NiCu and CoNi respectively on structural properties such as particle size, X-ray density and Dielectric Constant of Nanocrystalline spinel ferrite material.

II. MATERIALS AND METHODS

2.1. Experimental technique

In sol-gel auto combustion synthesis technique, high purity AR grade chemicals such as ferric nitrate (Fe(NO₃)₃·9H₂O), Copper nitrate (Cu(NO₃)₂·6H₂O), Nickel nitrate

(Ni(NO₃)₂·6H₂O), Cobalt nitrate (Co(NO₃)₂·6H₂O), citric acid (C₆H₈O₇), ammonium hydroxide solution (NH₄OH) were used to prepare the series of [(Ni_{0.2} Cu_{0.2}Co_{0.6})Fe₂O₄], [(Ni_{0.4} Cu_{0.2}Co_{0.4})Fe₂O₄], [(Ni_{0.6} Cu_{0.2}Co_{0.2})Fe₂O₄], [(Ni_{0.2} Cu_{0.6}Co_{0.2})Fe₂O₄], [(Ni_{0.2} Cu_{0.4}Co_{0.4})Fe₂O₄] and [(Ni_{0.4} Cu_{0.4}Co_{0.2})Fe₂O₄] Nano crystalline ferrite materials. In this chemical process Citric acid was used as a Fuel [8-10]. These nitrates and citric acid were weighed accurately to have proper stoichiometric proportion required in the final product. The mixed solutions of all the chemicals were stirred until the homogeneous solution is obtained. During the stirring process ammonium hydroxide solution was added drop by drop to obtain pH of 7. The mixed solution was simultaneously heated at 100 °C for 3 to 4 h to form sol. The transparent sol was further heated at 100 °C for 2 h for removal of water. The sol turns into a viscous brown gel. The temperature of the gel was further increased up to 120 °C, after some time combustion of the gel takes place and fine powder of ferrite nanoparticles was obtained. The ferrite powder was sintered at 400 °C for 4 hours in air medium to get better crystallization and homogeneous distribution in the spinel and finally ground to get the series of Nano crystalline ferrite material. **Table 1** indicates Label and composition for the series of ferrite materials of all six reactions which is divided in to three Sets.

The elemental stoichiometric coefficient, φ_e, is used to control the ratio of fuel to oxidizer in the reaction. φ_e represents the ratio between the oxidizing and reducing components of the metal nitrate fuel mixture. When φ_e is less than one (φ_e<1) it is fuel rich and when φ_e is greater than one (φ_e>1), the mixture does not have enough fuel for the completion of reaction. **Fig. 1** shows the flow chart of auto combustion synthesis used for the preparation of the ferrite powders and pellet.

2.2. Perpetration and Sintering of pellets

The pellets are prepared by mixing the polyvinyl alcohol (PVA) as binder in to ferrite powder. The mixed powder was uniaxially pressed by using a hydraulic press machine by applying the pressure of about 60 kg/cm³ for about 1 minute in a die of 10mm diameter. The final sintering of pellets was carried out at 200 °C for about 2 hours in air medium to densify the pellets. The pellets of diameter D_o-10 mm, thickness-2 mm are fabricated. The prepared samples of pellets were sintered in a furnace which uses electricity for heating the chamber with the help of super kanthal (MoSi₂) heating elements and alumina insulation boards as chamber walls. The dimension of chamber is 250x150x150 mm. The thermal regime of the furnace was controlled through a “Eurotherm” programmer-cum-controller designed by using microcontroller with an accuracy of ± 2 °C. The compacted samples heated from room temperature to 200 °C at a rate 1 °C/min followed by a soaking at 200 °C for 2 hours for binder burnout.

2.3. Characterization of Dielectric constant (ε)

The Dielectric constant (ε) of prepared samples was measured in the frequency range of 100 Hz to 5 MHz by using impedance analyser (LCR-Q Meter) meter at room temperature. The data acquisition system of digital impedance analyser (LCR-Q meter) provides the information of applied

frequency (f), measured Series Capacitance (Cs), Parallel Capacitance (Cp), Quality factor (Q).

The data provided by LCR-Q meter in addition to this data, thickness of pellet, d=0.002 meter, Diameter of pellet= 10 millimetre the Area of pellet = π r² = 3.14*.005*.005 meter²=0.0000785 meter² is used for calculations of Dielectric constant (ε). Following equations are used

Particle Size is calculated by using the formula,

$$t = \frac{0.9 \times \lambda}{\beta \times \cos \theta} \quad (1)$$

Where λ = Wave length of X-rays (CuKα₁ radiation=1.5418 Å)

t = Particle size.

θ = Bragg diffraction angle.

β = Full Width Half Maxima (FWHM) of the recorded peak θ and it is corrected for instrumental broadening.

The X-ray density obtained from molecular weight and volume of the unit cell by using the equation.

$$d_x = \frac{8M}{N_a a^3} \quad (2)$$

Where M is molecular weight, N_a is the Avogadro's number and 'a' is the lattice parameter.

Dielectric constant (Real Part) = ε = Cp × d/ε₀ × A – (3)

Table 2 shows Particle size, and X-ray density of all six ferrite materials. **Table 3** shows Avg. Dielectric constant (ε) for all Composition of Ferrite Material calculated in the frequency range of 100Hz to 5MHz at room temperature.

III. RESULTS AND DISCUSSION

3.1. X-ray diffraction pattern

Fig. 2 shows the X-ray diffraction pattern of SET-I (A, B & C). Its compositions exhibit single phase cubic spinel structure with Fd_{3m} space group and there is not presence of any secondary phase. All the reflections are slightly broader and less intense which indicate the nanocrystalline nature of the samples. The analysis of X-ray diffraction pattern revealed that all the samples under investigation possess single phase cubic spinel structure. XRD results confirm the formation of nanocrystalline ferrite material. Using the XRD data, the interplaner spacing 'd' values for all the reflections were determined using Bragg's law.

3.2. Effect of Ni²⁺ doping on Particle size

In Set-I, It is observed that due to the concentration of Ni²⁺ ions in place of Co²⁺ ions the Bragg's angle shifts towards higher angle and thereby interplaner spacing 'd' values decreases. The Particle size is found to decrease with increase in Ni²⁺ concentration x. The variations in Particle size as a function of Nickel concentration x can be understood on the basis of the ionic radius of the substituted Ni²⁺ ions. Since the ionic radius of Ni²⁺ ions (0.69 Å) is less than that of Co²⁺ ions (0.72 Å), the substitution is expected to decrease the Particle size with increase in Ni²⁺ concentration x. When the smaller nickel ions enters the lattice unit cell expands while preserving overall symmetry this is true as long as the Particle size decreases with substituent concentration. It can be seen from **Fig 3** that, the Particle size decreases with Ni²⁺ doping and obeys Vegard's law [11-14]. **Fig 4** shows that average

Dielectric constant decreases due to doping of Ni^{+2} . **Fig 3 and Fig 4** having correlation between Particle Size and average Dielectric constant due to doping of Ni^{+2} respectively. Whereas from **Fig 5** it is observed that X-ray density increases due to doping of Ni^{+2} .

3.3. Effect of Co^{2+} doping on Particle size

In Set-II, It is observed that due to the inclusion of Co^{2+} ions in place of Cu^{2+} ions the Bragg's angle shifts towards lower angle and thereby interplaner spacing 'd' values increases. **Fig 06** shows that Particle size increase with increase in Co^{2+} concentration x. The variations in Particle size as a function of Cobalt ions concentration x can be understood on the basis of the ionic radius of the substituted cations. Since the ionic radius of Co^{2+} ions (0.745Å) is greater than that of Cu^{2+} ions (0.73Å), the substitution is expected to increase the Particle size with increase in Cobalt doping x [15-17]. From **Fig 7 and Fig 08** it is observe that average Dielectric constant and X-ray density increases from 0.2 to 0.4 doping of Co^{2+} and thereafter both decreases for doping of Co^{2+} from 0.4 to 0.6 by showing the correlation between them.

When the larger Cobalt ions enters, the lattice unit cell expands while preserving overall symmetry this is true as long as the Particle size increases with doping Cobalt [18-19].

3.4 Effect of Cu^{2+} doping on Particle size

In Set – III, It is observed that due to the inclusion of Cu^{2+} ions in place of Ni^{2+} ions, from 0.2 to 0.4 the Bragg's angle shifts towards lower angle and thereby interplaner spacing 'd' values increases. From **Fig 09** it is observe that Particle size is increase with increase in Cu^{2+} doping from 0.2 to 0.4 and thereafter Particle size is found to decrease for further doping of Cu^{2+} from 0.4 to 0.6. The variations in Particle size as a function of Cu^{2+} doping can be understood on the basis of the ionic radius of the substituted Cu^{2+} ions. Since the ionic radius of Cu^{2+} ions (0.73Å) is greater than that of Ni^{2+} ions (0.69Å), the substitution is expected to increase the Particle size with increase in Copper concentration [20-22]. When the larger Copper ions enter, the lattice unit cell expands while preserving overall symmetry this is true as long as the Particle size increases with doping of Copper. **Fig 09 and Fig 11** show the correlation between Particle Size and X-ray density. **Fig 10** show that Average Dielectric Constant decrease with increase in Cu^{2+} doping from 0.2 to 0.4 and thereafter it increase for further doping of Cu^{2+} from 0.4 to 0.6.

3.5. Effect of Ni^{2+} ions doping on Dielectric constant (ϵ) sample A, B and C.

The Dielectric constant (ϵ) of all ferrite samples due to Ni^{2+} ions doping is calculated in the frequency range of 100 Hz to 5 MHz. The average of Dielectric constant (ϵ) of each sample is taken in to consideration for plotting the graph of Ni^{2+} ions doping (x=0.2, 0.4 & 0.6) verses average Dielectric constant (ϵ). From **Fig. 5** it is observed that average Dielectric constant (ϵ) decreases with increase of Ni^{2+} ions doping.

With the increase in the concentration of Ni^{2+} ions (x), the hopping action of charge carriers decreases due to the decreased concentration of Fe^{3+} ions at B-site, which results in decrease of average Dielectric constant.

3.6.Effect of Co^{2+} ions doping on Dielectric constant (ϵ) sample D, E and A.

The Dielectric constant (ϵ) of all ferrite samples due to Co^{2+} doping is calculated in the frequency range of 100 Hz to 5 MHz. The average of Dielectric constant (ϵ) of each sample is taken in to consideration for plotting the graph of Co^{2+} doping (x=0.2, 0.4 & 0.6) verses average Dielectric constant (ϵ).

From **Fig. 7** it is observed that with increase of Co^{2+} doping from 0.2 to 0.4 average Dielectric constant (ϵ) increases and thereafter it decreases with further increase of Co^{2+} doping from 0.4 to 0.6.

The decrease in Dielectric constant (ϵ) may be due to effect of decreased material composition of Cu^{2+} ions in SET-II.

3.7.Effect of Cu^{2+} ions doping on Dielectric constant (ϵ) sample C, F and D.

The Dielectric constant (ϵ) of all ferrite samples due to Cu^{2+} ions doping is calculated in the frequency range of 100 Hz to 5 MHz. The average of Dielectric constant (ϵ) of each sample is taken in to consideration for plotting the graph of Cu^{2+} ions doping (x=0.2, 0.4 & 0.6) verses average Dielectric constant (ϵ).

From **Fig.10** it is observed that with increase of Cu^{2+} doping from 0.2 to 0.4, average Dielectric constant (ϵ) decreases and thereafter it increases with further increase of Cu^{2+} doping from 0.4 to 0.6.

With the increase in the concentration of Cu^{2+} ions (x), the hopping action of charge carriers increases due to the increased concentration of Fe^{3+} ions at B-site.

It is well known that the mechanism of the electrical conduction is the same as that of the dielectric polarization [23-24].

The FTIR spectroscopy confirms the single phase nature of the prepared sample. The peak 536.114 cm^{-1} gives the confirmation of Fe_2O_4 . Fig. 8 shows the IR absorption peak at 536.114 cm^{-1} .

IV. LIST OF FIGUERS

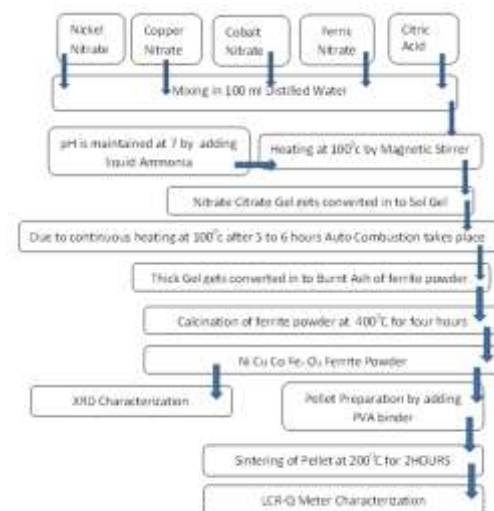


Fig.1: Flow Chart of SOL GEL for Ferrite Material and Pellet fabrication

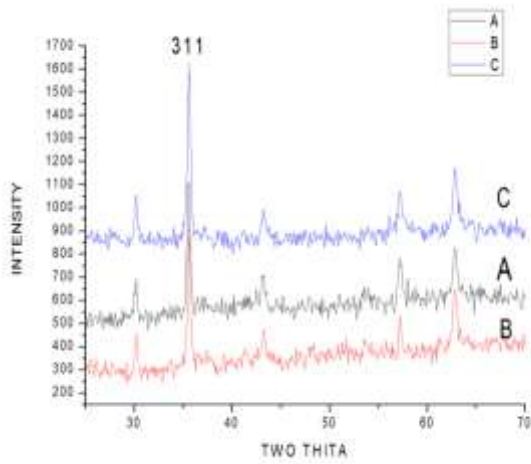


Fig. 2: XRD Pattern of SET-I ferrite samples

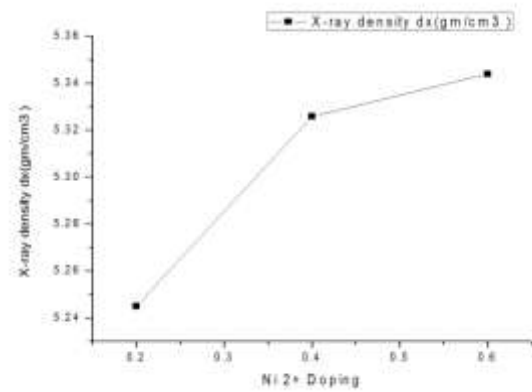


Fig. 5: Ni²⁺ doping versus X-ray density.

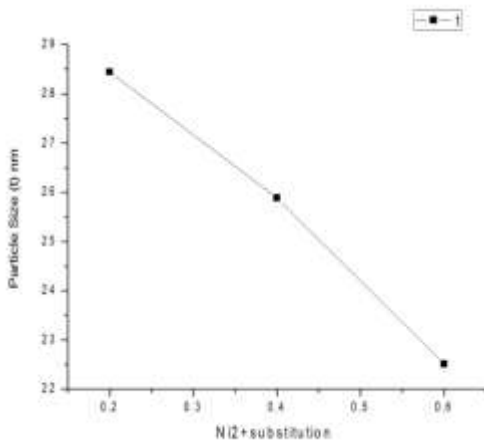


Fig. 3: Ni²⁺ doping versus particle size.

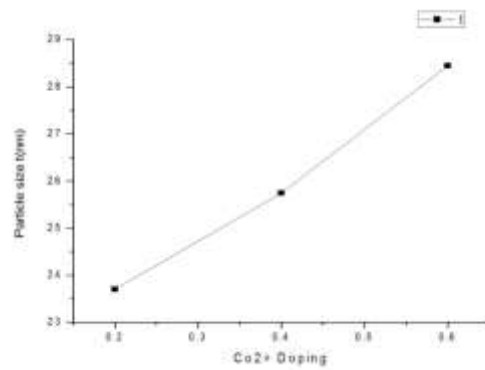


Fig. 6: Co²⁺ doping versus particle size.

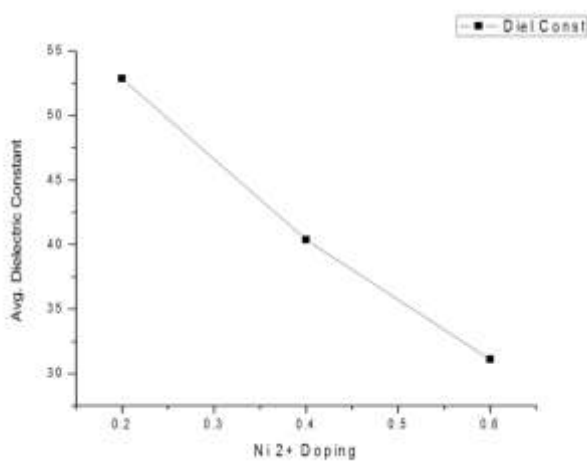


Fig. 4: Ni²⁺ doping versus Avg. dielectric constant.

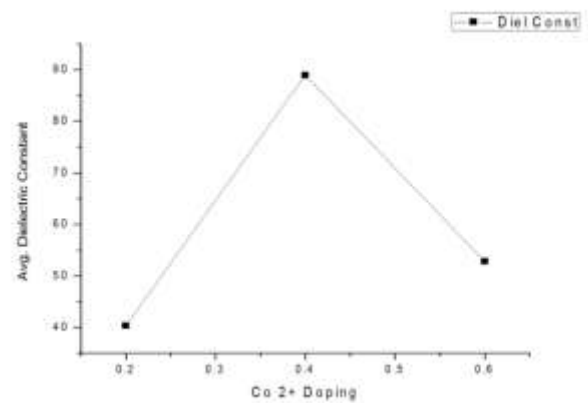


Fig. 7: Co²⁺ doping versus Avg. dielectric constant.

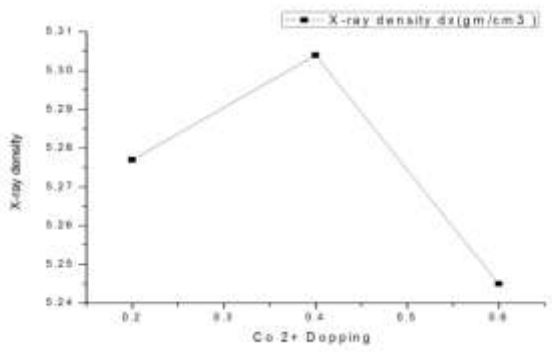


Fig.8: Co²⁺ doping versus X-ray density.

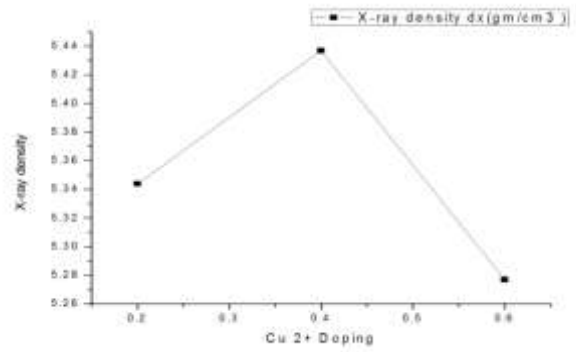


Fig. 11: Cu²⁺ doping versus X-ray density.

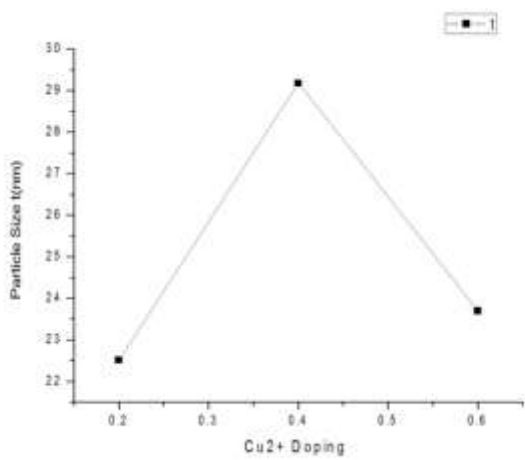


Fig. 09: Cu²⁺ doping versus particle size.

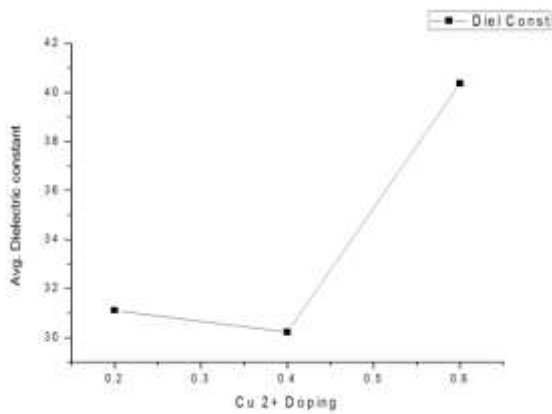


Fig. 10: Cu²⁺ doping versus Avg. dielectric constant.

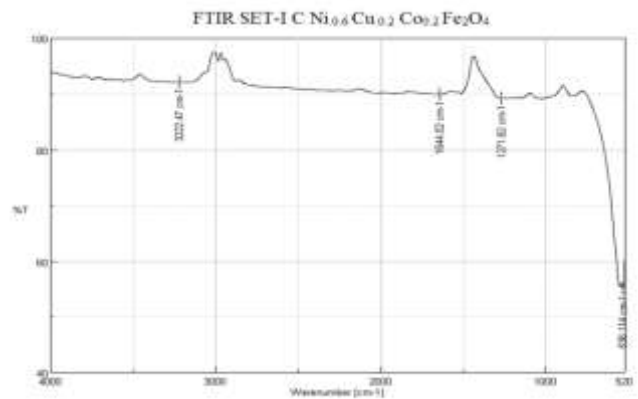


Fig. 12: FTIR graph for SET-I (C).

Table 1: Label and Composition of Ferrite Material.

SET	Label	Ferrite Material
SET-I	A	[(Ni _{0.2} Cu _{0.2} Co _{0.6})Fe ₂ O ₄]
	B	[(Ni _{0.4} Cu _{0.2} Co _{0.4})Fe ₂ O ₄]
	C	[(Ni _{0.6} Cu _{0.2} Co _{0.2})Fe ₂ O ₄]
SET-II	D	[(Ni _{0.2} Cu _{0.6} Co _{0.2})Fe ₂ O ₄]
	E	[(Ni _{0.2} Cu _{0.4} Co _{0.4})Fe ₂ O ₄]
	A	[(Ni _{0.2} Cu _{0.2} Co _{0.6})Fe ₂ O ₄]
SET-III	C	[(Ni _{0.6} Cu _{0.2} Co _{0.2})Fe ₂ O ₄]
	F	[(Ni _{0.4} Cu _{0.4} Co _{0.2})Fe ₂ O ₄]
	D	[(Ni _{0.2} Cu _{0.6} Co _{0.2})Fe ₂ O ₄]

Table 2: Particle Size(t) and X-ray density(dx)for allComposition of Ferrite Material.

Ferrite Sample	Particle Size t (nm)	X-ray density dx (gm/cm ³)
A=[(Ni _{0.2} Cu _{0.2} Co _{0.6})Fe ₂ O ₄]	28.45	5.245
B=[(Ni _{0.4} Cu _{0.2} Co _{0.4})Fe ₂ O ₄]	25.89	5.326
C=[(Ni _{0.6} Cu _{0.2} Co _{0.2})Fe ₂ O ₄]	22.52	5.344
D=[(Ni _{0.2} Cu _{0.6} Co _{0.2})Fe ₂ O ₄]	23.71	5.277
E=[(Ni _{0.2} Cu _{0.4} Co _{0.4})Fe ₂ O ₄]	25.75	5.304
F=[(Ni _{0.4} Cu _{0.4} Co _{0.2})Fe ₂ O ₄]	29.18	5.437

Table 3: Avg.Dielectric Constant for allComposition of Ferrite Material.

Ferrite Sample	Avg. Dielectric Constant
A= [(Ni _{0.2} Cu _{0.2} Co _{0.6})Fe ₂ O ₄]	52.907096
B= [(Ni _{0.4} Cu _{0.2} Co _{0.4})Fe ₂ O ₄]	40.394454
C= [(Ni _{0.6} Cu _{0.2} Co _{0.2})Fe ₂ O ₄]	31.122545
D= [(Ni _{0.2} Cu _{0.6} Co _{0.2})Fe ₂ O ₄]	40.372577
E= [(Ni _{0.2} Cu _{0.4} Co _{0.4})Fe ₂ O ₄]	88.997411
F= [(Ni _{0.4} Cu _{0.4} Co _{0.2})Fe ₂ O ₄]	30.233975

IV. CONCLUSION

We have successfully prepared six different types of Nanocrystalline Ferrite materials by successfully implementing Sol Gel Auto combustion method. All ferrite materials are having particle size in nanometer range and exhibit good Dielectric Constant property. These Ferrite materials can use as dielectric material in capacitors and in Microwave applications.

REFERENCES

- [1] C. G. Whinfrey, D. W. Eckort and A. Tauber, *J. Am. Chem. Soc.* 53 (1982) 2722
- [2] G.F. Goya, H.R. Rechenberg, Superparamagnetic transition and local-order in CuFe₂O₄ nanoparticles, *Nanostruct. Mater.* 10 (1998) 1001–1011.
- [3] C. Caizer, M. Stefanescu, *J. Phys. D. Appl. Phys.* 35 (2002) 3035
- [4] M.A. Ahmed, S.F. Mansour, M. Afifi, *J. Magn. Magn. Mater.* 324 (2012) 4-10
- [5] T. Jahanbin, M. Hashim, K. A. Mantori, *J. Magn. Magn. Mater.* 322(2010) 2684-2689.
- [6] P.S. Aghav, V.N. Dhage, M.L. Mane, D.R. Shengule, R.G. Dorik, K.M. Jadhav, *Physica B: Cond. Matter.* 406(2011) 4350
- [7] S. Sun, C.B. Murray, D. Weller, L. Folks, A. Moser, *Science* 287 (2000) 1989
- [8] T. Nakamura, Y. Okaro, Electromagnetic properties of Mn–Zn ferrite sintered ceramics, *J. Appl. Phys.* 79 (1996) 7129.
- [9] I.H. Gul, W. Ahmed, A. Maqsood, *J. Magn. Magn. Mater.* 320 (2008) 270–275
- [10] K. Byrappa, M. Yoshimura, Handbook of Hydrothermal Technology, Noyes Publications, New Jersey, USA, 2001.
- [11] P. Hermankova, M. Hermanek, R. Zboril, *Eur. J. Inorg. Chem.*, 2010, 1, 110.
- [12] J. Moulder, Handbook of X-ray Photoelectron Spectroscopy (XPS), USA 1995.
- [13] M.R. Anantharaman, S. Sindhu, S. Jagatheesan, K.A. Malini, P. Kurian, *J Phys. D* 32 (1999) 1801
- [14] D. L. Pavla, G. L. Lampman, G. S. Krlz, J. R. Vyvyan, Introduction to spectroscopy, Brooks/ coleengage learning, 2009.
- [15] K.W. Wagner, *Ann. Phys.* 40 (1913) 817.
- [16] I.T. Rabinkin, Z.I. Novikova, Ferrites, *Izv Acad. Nauk USSR, Minsk*, 1960.
- [17] J.C. Maxwell, Electricity and Magnetism, vol. 1, Oxford University Press, New York (1973), p. 1.
- [18] M. Penchal Reddy, W. Madhuri, N. Ramamanoher Reddy, K.V. Siva Kumar, V.R.K. Murthy, R. Ramakrishna Reddy, Influence of copper substitution on magnetic and electrical properties of MgCuZn ferrite prepared by microwave sintering method, *Mater. Sci. Eng. C* 30 (10) 1094–1099.
- [19] J. Du, Z. Liu, W. Wu, Z. Li, B. Han, Y. Huang, *Mater. Res. Bull.* 40 (2005) 928–935.
- [20] K J. Azadmanjiri, H.K. Salehani, M.R. Barati, F. Farzan, Preparation and electromagnetic properties of Ni_{1-x}Cu_xFe₂O₄ nanoparticle ferrites by sol–gel auto-combustion method, *Mater. Lett.* 61 (2007) 84–87.
- [21] M.A. Ahmed, S.F. Mansour, M. Afifi, *J. Magn. Magn. Mater.* 324 (2012) 4-10.
- [22] P.S. Aghav, V.N. Dhage, M.L. Mane, D.R. Shengule, R.G. Dorik, K.M. Jadhav, *Physica B: Cond. Matter.* 406(2011) 4350.
- [23] J. Jing, L. Liangchao, X. Feng, *J. Rare Earths* 25 (2007) 79.
- [24] J. Azadmanjiri, H.K. Salehani, M.R. Barati, F. Farzan, *Mater. Lett.* 61 (2007) 84–87.